Epistatic and independent functions of Caspase-3 and Bcl-X_L in developmental programmed cell death

K. A. Roth*†‡, C.-Y. Kuan*§, T. F. Haydar§, C. D'Sa-Eipper†, K. S. Shindler†, T. S. Zheng¶, K. Kuida‖, R. A. Flavell¶, and P. Rakic‡§

†Department of Pathology, Washington University School of Medicine, St. Louis, MO 63110; ¶Section of Immunobiology, Howard Hughes Medical Institute, and §Section of Neurobiology, Yale University School of Medicine, New Haven, CT 06510; and ‖Vertex Pharmaceuticals, Inc., Cambridge, MA 02139

Contributed by Pasko Rakic, November 2, 1999

The number of neurons in the mammalian brain is determined by a balance between cell proliferation and programmed cell death. Recent studies indicated that Bcl-X_L prevents, whereas Caspase-3 mediates, cell death in the developing nervous system, but whether Bcl-X_L directly blocks the apoptotic function of Caspase-3 *in vivo* is not known. To examine this question, we generated *bcl-x*/*caspase-3* double mutants and found that *caspase-3* deficiency abrogated the increased apoptosis of postmitotic neurons but not the increased hematopoietic cell death and embryonic lethality caused by the *bcl-x* mutation. In contrast, *caspase-3*, but not *bcl-x*, deficiency changed the normal incidence of neuronal progenitor cell apoptosis, consistent with the lack of expression of Bcl-X_L in the proliferative population of the embryonic cortex. Thus, although Caspase-3 is epistatically downstream to Bcl-X_L in postmitotic neurons, it independently regulates apoptosis of neuronal founder cells. Taken together, these results establish a role of programmed cell death in regulating the size of progenitor population in the central nervous system, a function that is distinct from the classic role of cell death in matching postmitotic neuronal population with postsynaptic targets.

Programmed cell death (apoptosis) is an important mechanism in mammalian nervous system development (1, 2). First, programmed cell death adjusts postmitotic neuron number to match the size of their peripheral targets (3). Second, early brain-region-specific apoptosis such as cell death in the lateral edges of the hindbrain neural fold is essential for normal neural tube closure (4). Finally, the incidence of apoptosis within the proliferative ventricular zones (VZ) suggests a potential role of programmed cell death in regulating the size of the progenitor pool (5). Given its importance in normal brain development, the mechanism of apoptosis has been a subject of active investigation.

Recent gene-targeting studies identified Bcl-X_L as a critical antiapoptotic factor and Bax, Apaf-1, Caspase-9, and Caspase-3 as key proapoptotic molecules during normal brain development (6–12). Mice lacking *bcl-x* die as embryos and experience massive death of hematopoietic cells and postmitotic neurons (6). In addition, Bcl-X_L-deficient neurons are markedly susceptible to trophic factor withdrawal *in vitro* (13). In contrast, mice lacking Bax show decreased cell death without obvious malformations (14), whereas targeted disruptions of *apaf-1*, *caspase-9*, or *caspase-3* lead to decreased neuronal apoptosis in the embryonic nervous system and gross structural abnormalities (8–12).

In the nematode *Caenorhabditis elegans*, the homologues of Bax (EGL-1), Bcl-X_L (CED-9), Apaf-1 (CED-4), and caspases (CED-3) have analogous effects on programmed cell death and form a linear cell death pathway (15). Thus, it is an intriguing possibility that Bax, Bcl-X_L, Apaf-1, Caspase-9, and Caspase-3 constitute an evolutionary conserved cell death pathway during brain development in mammals. Consistent with this hypothesis, it has been shown that *bax* deficiency prevents the increased cell death of immature neurons caused by the *bcl-x* mutation (16). Furthermore, null mutations of either *apaf-1* or *caspase-9* disrupt the activation of Caspase-3, indicating a linear epistatic relationship *in vivo* (8, 10). However, it remains unclear whether the antiapoptotic function of Bcl-X_L is mediated specifically through inhibition of the proapoptotic effects of Caspase-3.

To test this hypothesis directly, we introduced the *caspase-3* mutation into *bcl-x*-deficient mice to determine whether the (downstream) Caspase-3 deficiency would abolish the phenotypes of the (upstream) Bcl-X_L deficiency, as predicted by an epistatic relationship of these two molecules similar to their counterparts in *C. elegans* (17). In addition, we compared the embryonic expression pattern and null-mutation phenotypes of Bax, Bcl-X_L, and Caspase-3. Our results indicate that, although Caspase-3 is epistatically downstream to Bcl-X_L in postmitotic neurons, it has a unique effect on apoptosis of neuronal founder cells and is therefore pivotal for normal brain formation.

Materials and Methods

Generation of *bcl-x*/*caspase-3* Mutant Mice. To generate mice deficient in both Bcl-X_L and Caspase-3, double heterozygote (*bcl-x*$^{+/-}$/*caspase-3*$^{+/-}$) mice were bred to produce embryos of nine possible genotypes, including *bcl-x*$^{-/-}$/*caspase-3*$^{-/-}$ embryos. Endogenous and disrupted genes were detected by PCR analysis of tail DNA extracts as described (6, 12). To determine whether the distribution of generated genotypes followed the predicted Mendelian distribution, χ^2 analysis of contingency tables was used.

Quantification of Terminal Deoxynucleotidyltransferase-Mediated UTP End Labeling (TUNEL)-Positive Cells in Embryonic Day (E)12.5 Embryos. To detect DNA fragmentation during apoptosis, E12.5 embryos fixed in Bouin's fixative were cryoprotected in 30% (vol/vol) sucrose, frozen, and sectioned horizontally. Frozen 20-μm horizontal brain sections were incubated in 0.26 units/ml terminal deoxynucleotidyltransferase, 1× supplied buffer (Life Technologies), and 20 μM biotinylated-16-dUTP (Roche Molecular Biochemicals) for 60 min at 37°C. The sections were then rinsed, blocked with 2% (vol/vol) BSA in PBS (pH 7.4), and incubated with FITC-coupled streptavidin (Jackson ImmunoResearch; 1:100) in PBS.

Primary Telencephalic Culture. E12.5 telencephalic cells cultured in DMEM containing 1% FCS were incubated in 5% CO_2 at 37°C for 48 h as described (13). Propidium iodide was added to label dead cells, and cultures were fixed with Bouin's fixative for 20 min at 4°C. The numbers of total nuclei and propidium iodide

Abbreviations: TUNEL, terminal deoxynucleotidyltransferase-mediated UTP end labeling; E*n*, embryonic day *n*; PP, preplate region; VZ, ventricular zone; MZ, marginal zone; FB, forebrain.

*K.A.R. and C.-Y.K. contributed equally to this work.

‡To whom reprint requests should be addressed. E-mail: kroth@pathology.wustl.edu or pasko.rakic@yale.edu.

The publication costs of this article were defrayed in part by page charge payment. This article must therefore be hereby marked "*advertisement*" in accordance with 18 U.S.C. §1734 solely to indicate this fact.

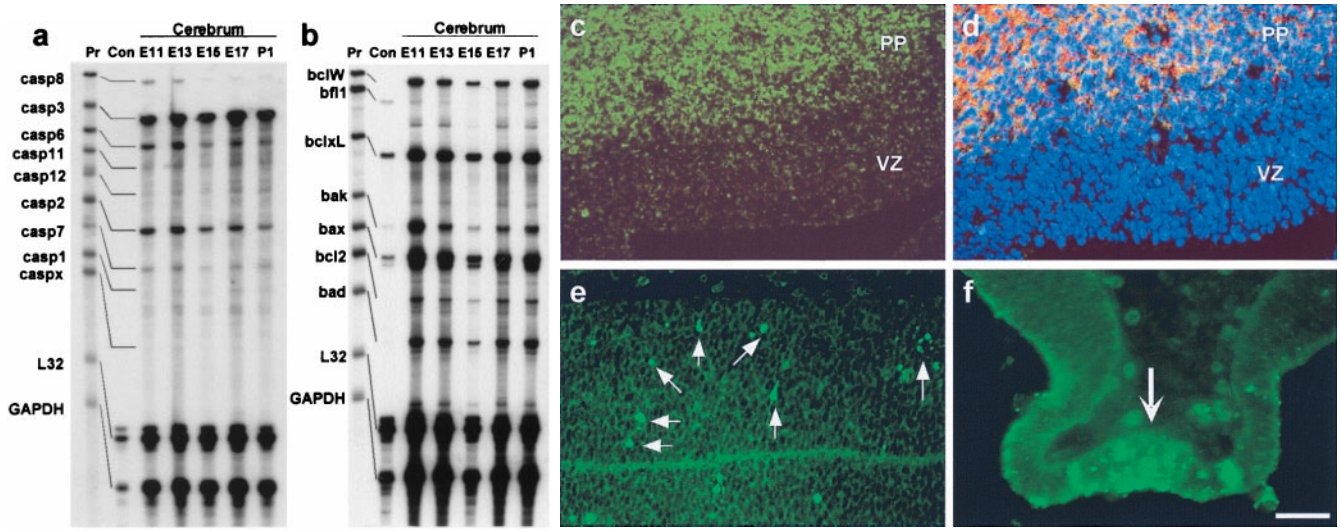

Fig. 1. Distinct expression patterns of Caspase-3 and Bcl-X_L in the developing mouse cerebrum. (*a* and *b*) RNase protection assay revealed strong expression of *caspase-3*, *bax*, and *bcl-x* in the mouse cerebrum from E11 to postnatal day (P) 1. Aliquots of the unprotected probes (Pr) and the RNase digestions with the control RNA supplied by the manufacturer (Con) were also run for comparison. Templates of the house-keeping genes L32 and glyceraldehyde-3-phosphate dehydrogenase (GAPDH) were included to indicate the amount of RNA loaded in each lane. (*c*) Immunocytochemistry indicates restricted expression of Bcl-X_L (green) in the preplate region (PP) of postmitotic neurons but not in the VZ of neuronal progenitor cells. (*d*) Triple bisbenzimide (blue), Bcl-X_L (green), and MAP2 (red) labeling of the E12.5 telencephalon indicated a colocalized expression (yellow) of Bcl-X_L and MAP2 in the PP. (*e* and *f*) Caspase-3 activation, as indicated by CM1 immunoreactivity (arrows), was found as early as E10.5 in telencephalic neuroepithelium (*e*) and laminal terminalis (*f*), suggesting a role in regulation of progenitor cell apoptosis. [Bar = 100 μm (*f*); 125 μm (*c* and *d*); and 200 μm (e).]

positive nuclei were counted at ×40 magnification from multiple randomly selected fields. Typically, between 150 and 200 nuclei were counted per well, and all conditions were performed in duplicate. Data from cultures were compared as percentages of total nuclei to control for slight differences in plating densities between embryos. Significance was established by using the nonparametric Kruskal–Wallis ANOVA on ranks and the Mann–Whitney rank sum test.

Histology and Immunocytochemistry. For semithin sections, 2% (vol/vol) glutaraldehyde-fixed embryos were embedded in plastic, and serial 1-μm sections were cut by a microtome. Of every 30 sections, 1 was collected and stained with 1% toluidine blue for detection of pyknotic nuclei. For immunocytochemistry, embryos were placed in Bouin's fixative overnight at 4°C, washed several times with 70% (vol/vol) ethanol, embedded in paraffin, and cut in 4-μm sagittal sections to be immunolabeled with antibodies to activated Caspase-3, MAP2, and Bcl-X_L by using described methods (18–22). Activated Caspase-3 was detected with an affinity-purified rabbit polyclonal antiserum, CM1, which recognizes the p18 subunit of cleaved Caspase-3 (18). Bcl-X_L immunoreactivity was detected with a mouse anti-Bcl-X_L monoclonal antibody (H5, Santa Cruz Biotechnology), and MAP2 immunoreactivity was detected with a monoclonal antibody (Sigma). The specificity of the H5 antibody was established, because no cross immunoreactivity was found in the *bcl-x*-deficient embryos. Activated Caspase-3, MAP2, and Bcl-X_L were detected with either fluorophore-conjugated secondary antibodies or the sequential tyramide signal amplification immunofluorescence methods (19–22). Tissue was counterstained with bisbenzimide and visualized on a Zeiss-Axioskop microscope equipped with epifluorescence.

RNase Protection Assay. A multiprobe template system (PharMingen) was used for the RNase protection assay. Total RNA (20 μg), prepared with the RNA-Stat 60 reagent (Tel-Test, Friendswood, TX), was used for each lane. The synthesis of [α-^{32}P]UTP-labeled probes by *in vitro* transcription and the RNase A/T1 digestion were carried out according to the manufacturer's instructions. The protected bands were resolved by electrophoresis in a 5% polyacrylamide gel and identified by calculation of the expected nucleotide length and the migration distance.

Results

Caspase-3 and Bcl-X_L Have Distinct Expression Patterns in Early Embryonic Brain. A ribonuclease protection assay was used to examine the expression of the caspase and Bcl-2 family genes during embryonic development of the mouse cerebrum. Expression of transcripts of *caspase-3*, *bcl-x*, and *bax* was detected as early as E11 until postnatal day 1 (Fig. 1 *a* and *b*). In addition to *caspase-3*, other effector caspases (*caspase-6*, *caspase-7*, and *caspase-2*) were also copiously expressed in the embryonic cerebrum throughout development.

Immunohistochemistry was used to localize the expression of Bcl-X_L and activated Caspase-3 in the mouse embryonic telencephalon. The expression of Bcl-X_L was found to be excluded from the proliferating population situated in the VZ but colocalized with a differentiated neuron marker (MAP2) in the PP of the E12.5 developing cerebrum (Fig. 1 *c* and *d*). In contrast, the activation of Caspase-3 was detected throughout the neuroepithelial wall including the proliferative VZ as early as E10.5 as seen by CM1 immunoreactivity (Fig. 1*e*), an antibody that recognizes the cleaved p18 fragment but not the 32-kDa proenzyme of Caspase-3 (18). In addition, the CM1 immunoreactivity was found greatly increased in specific brain regions, such as the laminal terminalia, characterized by high incidences of pyknotic clusters of dying cells (Fig. 1*f*). These results suggest that Caspase-3 may be involved in the apoptosis of neuronal founder cells and brain-region specific apoptosis, whereas Bcl-X_L is not.

Phenotypic Comparison Suggests That Caspase-3 Has a Unique Effect on Apoptosis of Neuronal Founder Cells Independent of the Functions of Bax and Bcl-X_L. The functions of Caspase-3, Bax, and Bcl-X_L in brain development were examined further and compared in E10.5 to E12.5 mutant embryos. In E12.5 wild-type embryos,

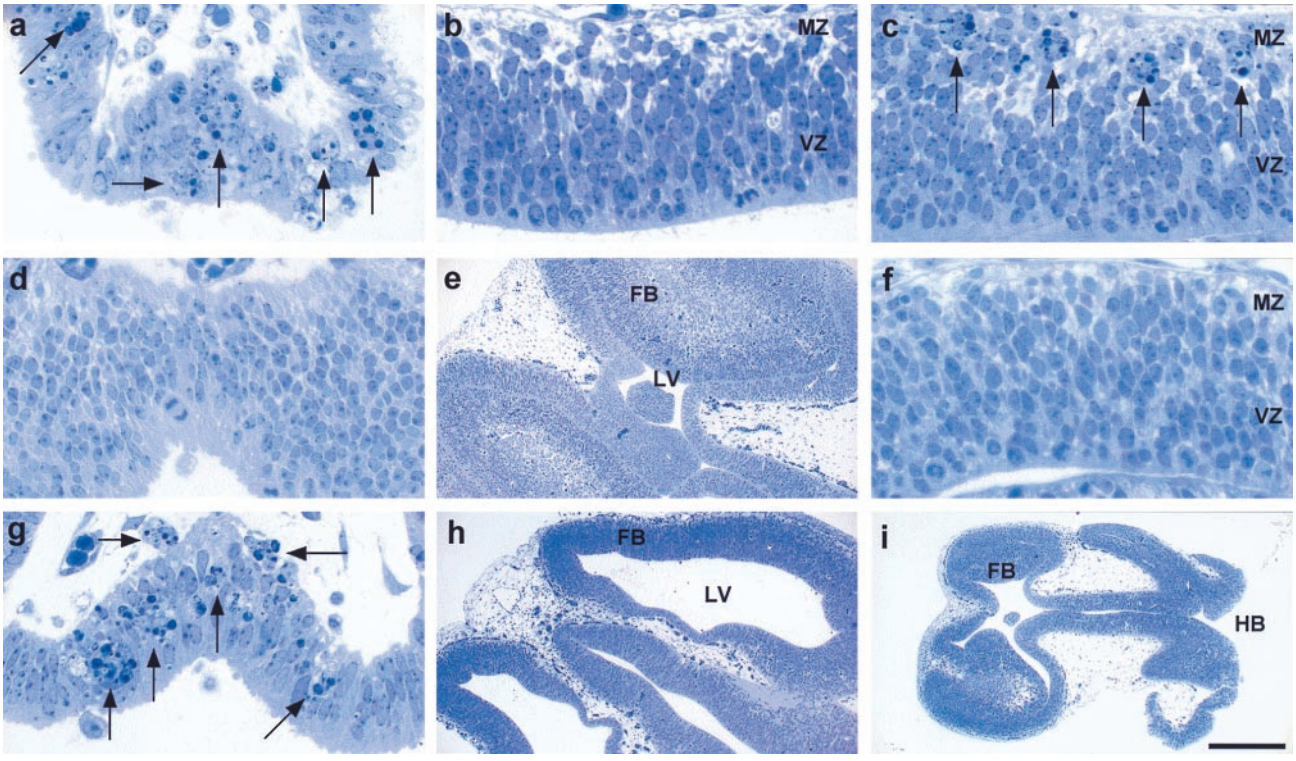

Fig. 2. Phenotypic comparison of developmental programmed cell death in E12.5 wild-type (*a* and *b*), *bcl-x* null-mutant (*c*), *caspase-3* null-mutant (*d* and *e*), *bax* null-mutant (*g* and *h*), and *bcl-x*/*caspase-3* double-null-mutant (*f* and *i*) brains. (*a*) In wild-type embryos, clusters of pyknotic cells (indicated by arrows) were confined to specific locations such as the lamina terminalis. (*b*) Besides these specific brain regions, very few pyknotic cells were found in the neuroepithelial wall, either in the proliferative VZ or in the postmitotic marginal zone (MZ), of the developing telencephalon. (*c*) In *bcl-x* mutant embryos, there were numerous ectopic pyknotic clusters (arrows) in the MZ of the developing cerebrum. (*d* and *e*) Region-specific pyknotic clusters such as in the lamina terminalis (*d*) were typically absent in *caspase-3* null-mutation embryos, which instead had supernumerary cells in the embryonic forebrain (FB) causing a severe reduction of the lateral ventricular (LV) space (*e*). (*g* and *h*) In contrast, the *bax* null-mutant embryos contained pyknotic clusters (arrows) in the lamina terminalis (*g*) and showed no signs of FB hyperplasia or reduction of the ventricular space (*h*). (*i*) Severe malformations of the nervous system similar to the phenotype of *caspase-3* deficiency, such as hindbrain (HB) exencephaly, were found in *bcl-x*/*caspase-3* double-mutant embryos. (*f*) Importantly, the abnormal pyknotic clusters detected in the developing cerebrum of *bcl-x* null mutants were totally eliminated by the concomitant *caspase-3* deficiency. [Bar = 2 mm (*i*); 1 mm (*e* and *h*); and 125 μm (*a*–*d*, *f*, and *g*).]

clusters of pyknotic cells were confined to specific brain regions such as the lamina terminalis (Fig. 2*a*) where intense CM1 immunoreactivity was also detected (Fig. 1*f*). Except for these specific brain regions, the developing neuroepithelial wall in wild-type embryos was largely devoid of pyknotic cells (Fig. 2*b*). In contrast, E12.5 *bcl-x*-deficient embryos had not only cell deaths in the laminal terminalis (data not shown) but also numerous ectopic pyknotic clusters in the MZ of the embryonic cerebrum where postmitotic neurons were located (Fig. 2*c*).

If Bax and Caspase-3 are both proapoptotic in an obligate, epistatic cell death pathway, the phenotype of *bax* deficiency should be identical to that of *caspase-3* deficiency. However, detailed analysis of mutant embryos revealed significant differences between the phenotypes of *bax*- and *caspase-3*-deficient embryos. The *caspase-3* deficiency caused the absence of apoptosis in the laminal terminalis (Fig. 2*d*) and marked hyperplasia of the embryonic nervous tissue (Fig. 2*f*). In contrast, brain-region-specific apoptosis was surprisingly preserved in the *bax*-deficient mutants (Fig. 2*g*). Moreover, there were no signs of hyperplasia or malformations of the nervous system in the *bax*-deficient embryos (Fig. 2*h*).

The effect of *caspase-3* deficiency on the apoptosis of postmitotic neurons was also examined by comparing TUNEL staining in the E12.5 telencephalon of *caspase-3*-deficient embryos with their wild-type littermates. The TUNEL assay revealed an uneven distribution of apoptotic cells in the embryonic telencephalon; TUNEL-positive cells were densely located within the lamina terminalis (24.07 ± 3.49; mean ± SEM; Fig. 3 *a* and *c*) and were correlated with high incidences of pyknotic cells observed in semithin sections (compare Fig. 2*a*). In contrast, only 18.3 ± 0.82 labeled cells per section were scattered throughout the rest of the FB (Fig. 3 *b* and *c*). For both areas of the brain, *caspase-3* deficiency caused a reduction of TUNEL-positive cells (1.6 ± 0.46 cells in the lamina terminalis and 4.4 ± 0.39 cells per section in the rest of the FB; Fig. 3*c*), suggesting a reduction of cell death of postmitotic neurons. However, it should be emphasized that, because recent studies indicated that cells may undergo apoptosis in the absence of Caspase-3 and without overt nuclear changes, a decrease of TUNEL-labeling in *caspase-3* mutant embryos may not reflect the actual reduction of cell death provided by Caspase-3 deficiency (refs. 23 and 24; R. W. Oppenheim, personal communication).

Caspase-3 Deficiency Does Not Prevent Increased Hematopoietic Cell Apoptosis or Embryonic Lethality in Bcl-X_L-Deficient Mice. To test directly the interaction between Caspase-3 and Bcl-X_L in development, we crossed heterozygous *bcl-x* and *caspase-3* mutant mice to generate *bcl-x* and *caspase-3* double-deficient animals. Genotypic analysis of 72 live-born pups derived from interbreeding of *bcl-x*$^{+/-}$/*caspase-3*$^{+/-}$ mice revealed no *bcl-x*$^{-/-}$/*caspase-3*$^{-/-}$ animals. In contrast, embryos harvested at E12.5, before the lethal effect of Bcl-X_L deficiency, had the expected ratio of genotype distribution according to Mendelian heredity (Table 1).

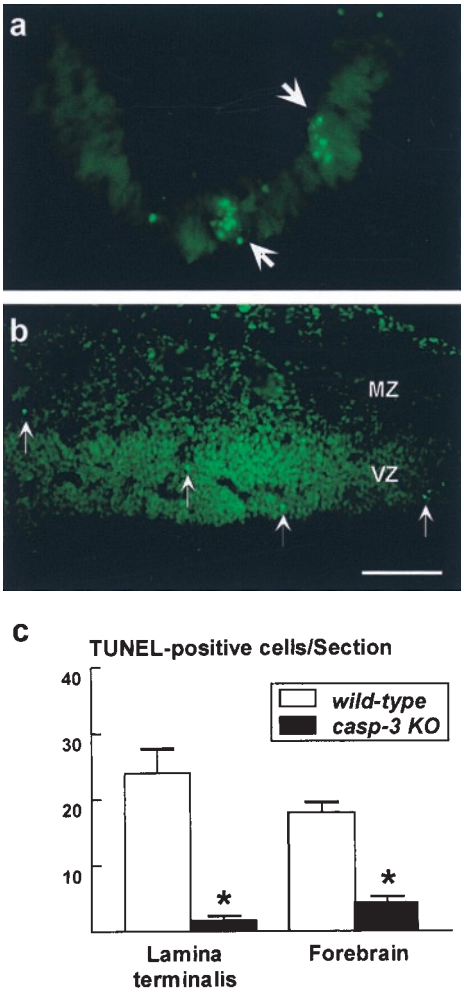

Fig. 3. Caspase-3 deficiency reduces TUNEL-positive apoptosis in developing brain. (*a* and *b*) TUNEL-positive apoptotic cells in the E12.5 telencephalon of wild-type embryos were densely concentrated in the lamina terminalis (*a*) but sparsely dispersed throughout the rest of the FB (*b*). (*c*) Quantification of TUNEL-positive cells in the E12.5 wild-type (white bars) and *caspase-3*$^{-/-}$ (black bars) telencephalon. Fewer TUNEL-positive cells are seen in the lamina terminalis and FB of the *caspase-3*-deficient brain. *, $P < 0.001$. [Bar = 125 μm (*a*) and 250 μm (*b*).]

The *bcl-x* deficiency results in embryonic lethality caused by increased apoptosis in the developing hematopoietic and/or hepatocellular system at ≈E13.5 (6). To determine the cause of embryonic lethality of the double mutants, the livers of E12.5 wild-type, *bcl-x*-deficient, *caspase-3*-deficient, and double-deficient embryos were examined by the TUNEL method and CM1 immunoreactivity. An ≈3-fold increase of TUNEL-positive cells was observed in the *bcl-x*-deficient liver, which was not reduced in the *bcl-x*$^{-/-}$/*caspase-3*$^{-/-}$ mutants (Table 2). Importantly, only rare CM1 immunoreactive cells were detected in the wild-type liver, which were not increased in the *bcl-x*-deficient liver (Table 2). This finding suggests that Bcl-X_L normally prevents a Caspase-3-independent apoptotic pathway in the developing hematopoietic system, the unchecked regulation of which is responsible for embryonic lethality of the *bcl-x*-deficient and *bcl-x*/*caspase-3* double-mutant embryos.

Caspase-3 Deficiency Abrogates Increased Apoptosis Caused by the Bcl-X_L Mutation Both *in Vivo* and *in Vitro*. Histological examination of the double mutants, however, indicates that the Caspase-3 deficiency is sufficient to eliminate virtually all ectopic apoptosis

Table 1. Genotypes of embryos and live-born mice generated from interbreeding of *bcl-x*$^{+/-}$/*casp3*$^{+/-}$ mice

Genotypes of offspring (expected frequency, %)	No. of E12.5 mice (%)	No. of live-born mice (%)
bcl-x$^{+/+}$/*casp3*$^{+/+}$ (6.25)	3 (6.7)	8 (11.1)
bcl-x$^{+/+}$/*casp3*$^{+/-}$ (12.5)	6 (13.3)	16 (22.2)
bcl-x$^{+/+}$/*casp3*$^{-/-}$ (6.25)	3 (6.7)	5 (6.9)
bcl-x$^{+/-}$/*casp3*$^{+/+}$ (12.5)	5 (11.1)	16 (22.2)
bcl-x$^{+/-}$/*casp3*$^{+/-}$ (25)	9 (22.0)	23 (31.9)
bcl-x$^{+/-}$/*casp3*$^{-/-}$ (12.5)	4 (8.9)	4 (5.6)
bcl-x$^{-/-}$/*casp3*$^{+/+}$ (6.25)	3 (6.7)	0 (0)*
bcl-x$^{-/-}$/*casp3*$^{+/-}$ (12.5)	7 (15.6)	0 (0)*
bcl-x$^{-/-}$/*casp3*$^{-/-}$ (6.25)	5 (11.1)	0 (0)*

E12.5 embryos ($n = 45$) and live-born mice ($n = 72$) were genotyped.
*These mice deviated significantly from the predicted Mendelian distribution based on χ^2 analysis of contingency.

caused by the *bcl-x* mutation in the nervous system. The E12.5 *bcl-x*$^{-/-}$/*caspase-3*$^{-/-}$ double mutants had gross brain malformations such as hindbrain exencephaly (Fig. 2*i*) previously reported in the *caspase-3* and *caspase-9* null mutations (10–12). In addition, the ectopic pyknotic clusters in the developing cerebrum caused by the Bcl-X_L deficiency were totally prevented by the additional Caspase-3 deficiency (Fig. 2*f*).

Similarly, although *bcl-x*-deficient embryos showed a marked increase of apoptotic cells in the spinal cord as compared with wild-type mice (Fig. 4*a*), this aberrant neuronal apoptosis was rescued by the additional *caspase-3* deficiency in the double mutants (Fig. 4*b*). The suppression of cell death in the double-mutant spinal cord correlated with an absence of activated Caspase-3-positive cells (Fig. 4 *c* and *d*). Furthermore, quantitative analysis of TUNEL-positive and CM1-immunoreactive cells in the dorsal root ganglia indicated that both apoptosis and Caspase-3 activation are suppressed in the *bcl-x*$^{-/-}$/*caspase-3*$^{-/-}$ mutants compared with *bcl-x*$^{-/-}$ mutants (Table 2). Together, these results indicate that *bcl-x* deficiency causes apoptosis of postmitotic neurons primarily through uninhibited activation of Caspase-3 *in vivo*.

Primary telencephalic cell cultures were used to define further the interaction between Bcl-X_L and Caspase-3 in postmitotic neurons, because Bcl-X_L-deficient neurons are markedly susceptible to apoptosis *in vitro* (13). Telencephalic cells isolated from E12.5 wild-type, *bcl-x*-deficient, *caspase-3*-deficient, and double-deficient embryos were grown for 48 h in DMEM

Table 2. Apoptosis and Caspase-3 activation in E12.5 liver and dorsal root ganglia

	Liver, cells per field		Dorsal root ganglia, cells per field	
Genotype	TUNEL	CM1	TUNEL	CM1
bcl-x$^{+/*}$/*casp3*$^{+/*}$	11 ± 1.3	0.28 ± 0.04	6.9 ± 0.7	6.9 ± 0.4
bcl-x$^{-/-}$/*casp3*$^{+/*}$	32 ± 2.7†	0.36 ± 0.10	16.8 ± 1.4†	21.2 ± 1.4†
bcl-x$^{+/*}$/*casp3*$^{-/-}$	14 ± 2.7	0.08 ± 0.03	1.8 ± 0.7†	0 ± 0†
bcl-x$^{-/-}$/*casp3*$^{-/-}$	31 ± 3.3†	0.14 ± 0.08	3.0 ± 0.9†	0.05 ± 0.05†

TUNEL- and CM1-positive cells were quantified in multiple ×60 magnification fields of liver and dorsal root ganglia from each embryo. The mean number of positive cells and SEM per field were determined for each group. Significance was determined by using the nonparametric Kruskal–Wallis ANOVA on ranks. The numbers of embryos used for both TUNEL and CM1 immunoreactivity in each genotype are *bcl-x*$^{+/*}$/*casp3*$^{+/*}$ (23/14); *bcl-x*$^{-/-}$/*casp3*$^{+/*}$ (10/4); *bcl-x*$^{+/*}$/*casp3*$^{-/-}$ (7/4); and *bcl-x*$^{-/-}$ (5/4). $^{+/*}$/*casp3*$^{-/-}$ includes both $^{+/+}$ and $^{+/-}$ mice. †, $P < 0.05$ compared to *bcl-x*$^{+/*}$/*casp3*$^{+/*}$ mice.

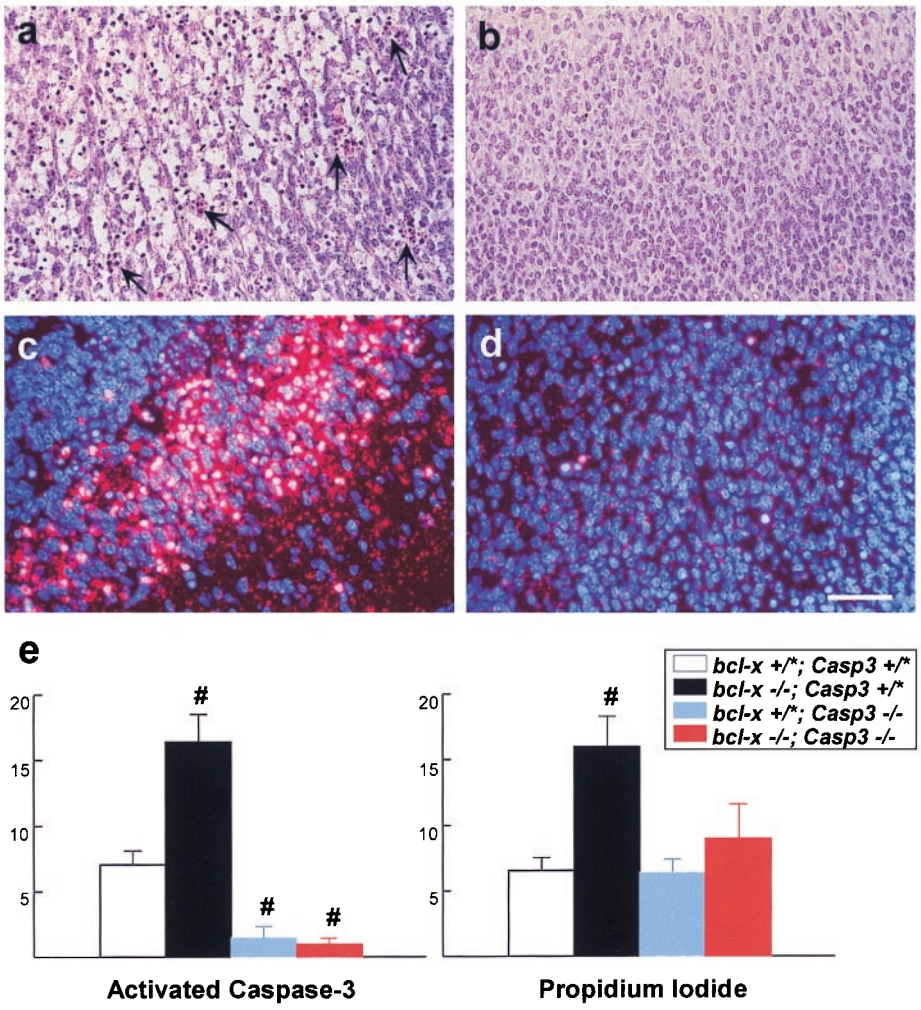

Fig. 4. Caspase-3 deficiency suppresses the increased neuronal apoptosis caused by Bcl-X_L deficiency. (*a–d*) The E12.5 *bcl-x*$^{-/-}$/*caspase-3*$^{+/+}$ spinal cord contained numerous pyknotic clusters (arrows) and sheets of apoptotic neurons in the Nissl stain (*a*), which were correlated with extensive Caspase-3 activation (*c*) as indicated by dual label of bisbenzimide (blue) and CM1 immunoreactivity (red). In contrast, ectopic pyknosis and CM1 immunoreactivity were eliminated in the E12.5 *bcl-x*$^{-/-}$/*caspase-3*$^{-/-}$ spinal cord (*b* and *d*). [Bar = 50 μm (*a–d*).] (*e*) Quantification of Caspase-3 activation and cell death in control, *bcl-x*$^{-/-}$, *caspase-3*$^{-/-}$, and *bcl-x*$^{-/-}$/*caspase-3*$^{-/-}$ E12.5 telencephalic cells grown for 48 h in DMEM plus 1% FCS; Caspase-3 activation was detected with CM1 antiserum, and cell viability was determined by exclusion of propidium iodide. Bcl-X_L-deficient cells had increased Caspase-3 activation and cell death; concomitant Caspase-3 deficiency inhibited the death-promoting effects of Bcl-X_L deficiency in this *in vitro* paradigm. No effect of gene dosage on neuronal apoptosis was observed for either *bcl-x* or *caspase-3*, and therefore, data from wild-type and heterozygous mutants were pooled (* denotes either $^+$ or $^-$). #, $P < 0.05$ compared with *bcl-x*$^{+/*}$/*caspase-3*$^{+/*}$ cells.

containing 1% FCS and then stained with propidium iodide to identify nonviable cells. After fixation, CM1 immunocytochemistry was performed to detect Caspase-3 activation (Fig. 4*e*). The Bcl-X_L-deficient telencephalic neurons had increased Caspase-3 activation and greater cell death compared with wild-type neurons. However, double-mutant cells grown in DMEM with 1% FCS had reduced cell death correlated with little Caspase-3 activation (Fig. 4*e*). Together, these *in vitro* results are consistent with the ability of *caspase-3* deficiency to rescue *bcl-x*-deficient neurons from apoptotic cell death *in vivo* and further support an epistatic relationship between Bcl-X_L and Caspase-3 in postmitotic neurons.

Discussion

Recent gene-targeting studies indicated that Bcl-X_L prevents, whereas Bax and Caspase-3 promote, cell death in the developing nervous system (6, 12, 14). It has been shown that *bax* deficiency prevents the increased cell death of postmitotic neurons in *bcl-x*-deficient embryos, suggesting an epistatic interaction between Bax and Bcl-X_L in brain development (16). In the present study, we examined the interaction between Bcl-X_L and Caspase-3 by analyzing mice carrying targeted gene disruptions in one or both of these molecules. Our results indicate that Caspase-3 mediates apoptosis of both founder cells and postmitotic neurons, whereas Bcl-X_L functions as an antiapoptotic factor exclusively in the postmitotic population. Importantly, the proapoptotic function of Caspase-3 in founder cells is unique and not shared by Bax. Moreover, the additional Caspase-3 deficiency abrogates the increased apoptosis of postmitotic neurons caused by the absence of Bcl-X_L both *in vivo* and *in vitro*. These results provide definitive genetic evidence that, in postmitotic neurons in the developing mammalian nervous system, Bcl-X_L and Caspase-3 form an obligate cell death pathway, similar to their homologues in the nematode *C. elegans*.

We propose a scheme to explain the interactions of Bax, Bcl-X_L, and Caspase-3 during mammalian brain development (Fig. 5). Bcl-X_L inhibits the proapoptotic effect of Caspase-3 in the postmitotic neuronal population (Fig. 5, actions a and b), and

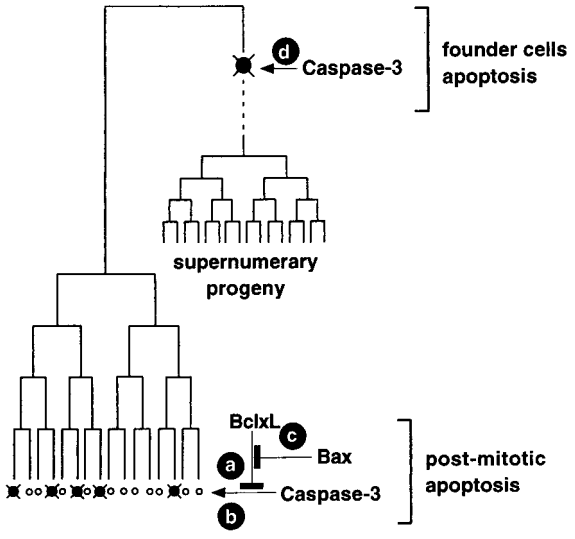

Fig. 5. Epistatic and independent apoptotic functions of Caspase-3 and Bcl-X_L in the developing mammalian nervous system. (Actions a–c) Bax, Bcl-X_L, and Caspase-3 form an epistatic pathway in the apoptosis of postmitotic neurons. (Action d) Caspase-3 regulates selective apoptosis of the neuronal founder cells. Inhibition of the progenitor cell apoptosis thus results in supernumerary progeny and brain malformations.

therefore *bcl-x* deficiency causes increased apoptosis of postmitotic neurons (6), which is prevented by the additional absence of *caspase-3*. Bax seems to modulate the antiapoptotic effects of Bcl-X_L (Fig. 5, action c); the null mutation of *bax* therefore reduces the normally occurring developmental death of postmitotic neurons without affecting the global formation of the nervous system (14).

The distinguishing characteristic of Caspase-3 in this scheme is its dual functions in both postmitotic and neuronal progenitor apoptosis (Fig. 5, actions b and d). Although *caspase-3* deficiency results in decreased apoptosis of postmitotic neurons in the developing cortex, given the normal brain structures in *bax*-deficient mice, this effect is unlikely to be sufficient to cause gross malformations. Instead, the unique effect of caspases on progenitor cell apoptosis is critical for establishing the size of the neuronal founder pool (25). Deficiency of Caspase-3 thus rescues a number of progenitor cells from programmed cell death, resulting in an exponential expansion of the progeny, ultimately leading to marked dysplasia and malformations of the nervous system. Therefore, these results suggest that programmed cell death is not only important for adjusting the final number of neurons to match their target fields but is also essential for establishing the initial size of the progenitor pool in the developing nervous system.

We thank C. Latham, J. McDonough, B. Klocke, J. Musco, and J. Bao for technical assistance; A. Whitmarsh for advice on the RNase protection assay; and A. Schroeder for secretarial support. Bcl-x- and Bax-deficient mice were generously provided by Dennis Y. Loh, and CM1 antiserum was provided by Anu Srinivasan (IDUN Pharmaceuticals, Inc.). R.A.F. is an investigator of the Howard Hughes Medical Institute. This work was supported by grants from the National Institutes of Health to K.A.R. and P.R.

1. Glucksmann, A. (1951) *Biol. Rev.* **26,** 58–86.
2. Oppenheim, R. W. (1991) *Annu. Rev. Neurosci.* **14,** 453–501.
3. Jacobson, M. D., Weil, M. & Raff, M. C. (1997) *Cell* **88,** 347–354.
4. Kuan, C.-Y., Yang, D. D., Samanta Roy, D. S., Davis, R. J., Rakic, P. & Flavell, R. A. (1999) *Neuron* **22,** 667–667.
5. Thomaidou, D., Mione, M. C., Cavanagh, J. F. R. & Parnavelas, J. G. (1997) *J. Neurosci.* **17,** 1075–1085.
6. Motoyama, N., Wang, F., Roth, K. A., Sawa, H., Nakayama, K.-I., Nakayama, K., Negishi, I., Senju, S., Zhang, Q., Fujii, S., *et al*. (1995) *Science* **267,** 1506–1510.
7. Knudson, C. M., Tung, K. S. K., Tourtellotte, W. G., Brown, G. A. J. & Korsmeyer, S. J. (1995) *Science* **270,** 96–99.
8. Cecconi, F., Alvarez-Bolado, G., Meyer, B. I., Roth, K. A. & Gruss, P. (1998) *Cell* **94,** 727–737.
9. Yoshida, H., Kong, Y.-Y., Yoshida, R., Elia, A. J., Hakem, A., Hakem, R., Penninger, J. M. & Mak, T. W. (1998) *Cell* **94,** 739–750.
10. Kuida, K., Haydar, T. F., Kuan, C.-Y., Gu, Y., Taya, C., Karasuyama, H., Su, M. S.-S., Rakic, P. & Flavell, R. A. (1998) *Cell* **94,** 325–337.
11. Hakem, R., Hakem, A., Duncan, G. S., Henderson, J. T., Woo, M., Soengas, M. S., Elia, A., de la Pompa, J. L., Kägi, D., Shoo, W., *et al*. (1998) *Cell* **94,** 339–352.
12. Kuida, K., Zheng, T. S., Na, S., Kuan, C.-Y., Yang, D., Karasuyama, H., Rakic, P. & Flavell, R. A. (1996) *Nature (London)* **384,** 368–382.
13. Roth, K. A., Motoyama, N. & Loh, D. Y. (1996) *J. Neurosci.* **16,** 1753–1758.
14. White, F. A., Keller-Peck, C. R., Knudson, C. M., Korsmeyer, S. J. & Snider, W. D. (1998) *J. Neurosci.* **18,** 1428–1439.
15. Metzstein, M. M., Stanfield, G. M. & Horvitz, H. R. (1998) *Trends Genet.* **14,** 410–416.
16. Shindler, K. S., Latham, C. B. & Roth, K. A. (1997) *J. Neurosci.* **17,** 3112–3119.
17. Hengartner, M. O., Ellis, R. E. & Horvitz, H. R. (1992) *Nature (London)* **356,** 494–499.
18. Srinivasan, A., Roth, K. A., Sayers, R. O., Shindler, K. S., Wong, A. M., Fritz, L. C. & Tomaselli, K. J. (1998) *Cell Death Differ.* **5,** 1004–1016.
19. Flaris, N. A., Shindler, K. S., Kotzbauer, P. T., Chand, P., Ludwig, C. P., Konstantinidou, A. D. & Roth, K. A. (1995) *Brain Res.* **678,** 99–109.
20. Shindler, K. S. & Roth, K. A. (1996) *Dev. Brain Res.* **92,** 199–210.
21. Tornusciolo, D. R. Z., Schmidt, R. E. & Roth, K. A. (1995) *BioTechniques* **19,** 800–809.
22. Shindler, K. S. & Roth, K. A. (1996) *J. Histochem. Cytochem.* **11,** 1331–1335.
23. D'Mello, S. R., Kuan, C.-Y., Flavell, R. A. & Rakic, P. (2000) *J. Neurosci. Res.*, in press.
24. Zheng, T. S., Schlosser, S. F., Dao, T., Hingorani, R., Crispe, I. N., Boyer, J. L. & Flavell, R. A. (1998) *Proc. Natl. Acad. Sci. USA* **95,** 13618–13623.
25. Haydar, T. F., Kuan, C.-Y., Flavell, R. A. & Rakic, P. (1999) *Cereb. Cortex* **9,** 621–626.